GEOPHYSICAL RESEARCH LETTERS, VOL. 35, L12606, doi:10.1029/2008GL033669, 2008

Probability distribution function of the upper equatorial Pacific current speeds

Peter C. Chu[1]

Received 15 February 2008; revised 4 April 2008; accepted 17 April 2008; published 28 June 2008.

[1] The probability distribution function (PDF) of the upper (0–50 m) tropical Pacific current speeds (w), constructed from hourly ADCP data (1990–2007) at six stations for the Tropical Atmosphere Ocean project, satisfies the two-parameter Weibull distribution reasonably well with different characteristics between El Nino and La Nina events: In the western Pacific, the PDF of w has a larger peakedness during the La Nina events than during the El Nino events; and vice versa in the eastern Pacific. However, the PDF of w for the lower layer (100–200 m) does not fit the Weibull distribution so well as the upper layer. This is due to the different stochastic differential equations between upper and lower layers in the tropical Pacific. For the upper layer, the stochastic differential equations, established on the base of the Ekman dynamics, have analytical solution, i.e., the Rayleigh distribution (simplest form of the Weibull distribution), for constant eddy viscosity K. Knowledge on PDF of w during the El Nino and La Nina events will improve the ensemble horizontal flux calculation, which contributes to the climate studies. **Citation:** Chu, P. C. (2008), Probability distribution function of the upper equatorial Pacific current speeds, *Geophys. Res. Lett.*, *35*, L12606, doi:10.1029/2008GL033669.

1. Introduction

[2] Tropical Pacific Ocean contributes significantly to the global redistribution of heat necessary to maintain the earth's thermal equilibrium. For example, the El Niño (La Nina) phenomenon, an eastward (westward) shift of warm (cool) water, is a key component of global interannual climate variability. In connection with the El Nino and La Nina phenomena, impact of upper tropical Pacific on global climate changes has attracted large attention. During the El Nino or La Nina event, equatorial currents take an active role in redistribution of heat that changes the sea surface temperature (SST) and in turn affects the atmospheric general circulations.

[3] Surface layer horizontal fluxes of momentum, heat, water mass and chemical constituents are typically nonlinear in the speed [*Lozano et al.*, 1996; *Galanis et al.*, 2005], so the space or time average flux is not generally equal to the flux that would be diagnosed from the averaged current speed. In fact, the average flux will generally depend on higher-order moments of the current speed, such as the standard deviation, skewness, and kurtosis. From both diagnostic and modeling perspectives, there is a need for parameterizations of the probability distribution function (PDF) of the current speed w (called w-PDF here).

[4] The w-PDF has been investigated thoroughly in the atmosphere. For example, the w-PDF for the surface winds is well represented by the two-parameter Weibull distribution [e.g., *Monahan*, 2006]. However, the w-PDF has not been investigated in the oceans. To fill this gap, we use hourly Acoustic Doppler Current Profiler (ADCP) data (1990–2007) at all the six stations during the Tropical Atmosphere Ocean (TAO) project [*McPhaden et al.*, 1998] in this study to construct the observational w-PDF for various layers. The purpose is to identify which theoretical PDF should be used for the current speed for general and/or special events such as El Nino and La Nina. Special characteristics of the statistical parameters such as mean, standard deviation, skewness, and kurtosis will also be identified. The rest of the paper is organized as follows. Section 2 describes the data. Section 3 presents theoretical background for determining the w-PDF for upper oceans. Section 4 shows the basic characteristics of the four parameters of the Weibull distribution. Section 5 constructs the observational w-PDF from the TAO-ADCP data and discusses the basic features of the four parameters. Section 6 presents the conclusions.

2. Data

[5] The upper layer ocean current dataset consists of hourly ADCP moorings from the TAO project at the six stations (147°E, 156°E, 165°E, 170°W, 140°W, 110°W) along the equator with the vertical resolution of 5 m. Temporal data coverage varies from station to station: 1993–2004 with interruptions during 1997–1998 and 2001–2003 on 147°E, 1990–1995 on 156°E, 1990–2007 with interruption during 1993–1994 on 165°E, 1999–2006 with interruption 1992–1993 on 170°W, 1995–2007 on 140°W, and 1995–2007 with interruption in 2004 on 110°W. The hourly horizontal velocity data (u, v) can be downloaded from the website: http://www.pmel.noaa.gov/tao/. The current speed (w) is calculated from (u, v).

3. Theoretical Background

[6] Let (x, y) be the horizontal coordinates and z be the vertical coordinate. The corresponding horizontal velocity components are represented by ($\tilde{u}$, $\tilde{v}$). Large-scale horizontal momentum equation is written by

$$\frac{\partial \tilde{u}}{\partial t} - f\left(\tilde{v} - v_g\right) = \frac{1}{\rho}\frac{\partial X}{\partial z}, \tag{1}$$

$$\frac{\partial \tilde{v}}{\partial t} + f\left(\tilde{u} - u_g\right) = \frac{1}{\rho}\frac{\partial Y}{\partial z}, \tag{2}$$

[1]Department of Oceanography, Naval Postgraduate School, Monterey, California, USA.

where (X, Y) are the horizontal stresses; p is the pressure; ρ is the density; f is the Coriolis parameter; and (u_g, v_g) are geostrophic velocity components defined by

$$u_g = -\frac{1}{f\rho}\frac{\partial p}{\partial y}, \quad v_g = \frac{1}{f\rho}\frac{\partial p}{\partial x}. \tag{3}$$

[7] Integrating (1) and (2) from the ocean surface ($z = 0$) to a constant scale depth (h) of surface mixed layer leads to

$$\frac{\partial U}{\partial t} - fV_E = \frac{1}{\rho}(X_0 - X_{-h}), \tag{4}$$

$$\frac{\partial V}{\partial t} + fU_E = \frac{1}{\rho}(Y_0 - Y_{-h}), \tag{5}$$

where

$$(U, V) = \int_{-h}^{0} (\tilde{u}, \tilde{v})dz = (hu, hv), \tag{6}$$

$$(U_E, V_E) = \int_{-h}^{0} (\tilde{u} - u_g, \tilde{v} - v_g)dz, \tag{7}$$

with (u, v) the vertical means of ($\tilde{u}$, $\tilde{v}$), (X_0, Y_0) = (τ_x, τ_y) the surface wind stress components; and (X_{-h}, Y_{-h}) the stress components at $z = -h$, which is calculated by

$$\frac{X_{-h}}{\rho} \approx -\frac{K}{h}u, \quad \frac{Y_{-h}}{\rho} \approx -\frac{K}{h}v. \tag{8}$$

[8] Here, we assume that the horizontal velocity is much weaker below the mixed layer than in the mixed layer. K is the eddy viscosity. Substitution of (6)–(8) into (4) and (5) gives

$$\frac{\partial u}{\partial t} = \frac{1}{h}\Lambda_u - \frac{K}{h^2}u, \tag{9}$$

$$\frac{\partial v}{\partial t} = \frac{1}{h}\Lambda_v - \frac{K}{h^2}u, \tag{10}$$

where

$$\Lambda_u \equiv fV_E + \frac{\tau_x}{\rho}, \quad \Lambda_v \equiv -fU_E + \frac{\tau_y}{\rho} \tag{11}$$

represent the residual between the Ekman transport and surface wind stress. With absence of horizontal pressure gradient, e.g., $u_g = v_g = 0$, Equations (9) and (10) reduce to the commonly used wind-forced slab model [e.g., *Pollard and Millard*, 1970],

$$\frac{\partial u}{\partial t} = fv + \frac{\tau_x}{\rho h} - \frac{K}{h^2}u$$

$$\frac{\partial v}{\partial t} = -fu + \frac{\tau_y}{\rho h} - \frac{K}{h^2}v.$$

[9] For the sake of convenience, we assume that the residual between the Ekman transport (U_E, V_E) and surface wind stress does not depend on the horizontal current vector (u, v). Away from the equator, this approximation is similar to a small Rossby number approximation [*Gill*, 1982]. If the forcing (Λ_u, Λ_v) is fluctuating around some mean value,

$$\Lambda_u(t) = \langle\Lambda_u\rangle + \dot{W}_1(t)h\Sigma, \quad \Lambda_v(t) = \langle\Lambda_v\rangle + \dot{W}_2(t)h\Sigma, \tag{12}$$

where the angle brackets represent ensemble mean and the fluctuations are taken to be isotropic and white in time:

$$\left\langle \dot{W}_i(t_1)\dot{W}_j(t_2)\right\rangle = \delta_{ij}\delta(t_1 - t_2), \tag{13}$$

with a strength that is represented by Σ. Note that the Ekman transport is determined by the surface wind stress for time-independent case, and therefore the ensemble mean values of (Λ_u, Λ_v) are zero,

$$\langle\Lambda_u\rangle = 0, \quad \langle\Lambda_v\rangle = 0. \tag{14}$$

[10] Substitution of (12)–(14) into (9) and (10) gives

$$\frac{\partial u}{\partial t} = -\frac{K}{h^2}u + \dot{W}_1(t)\Sigma, \tag{15}$$

$$\frac{\partial v}{\partial t} = -\frac{K}{h^2}v + \dot{W}_2(t)\Sigma, \tag{16}$$

which is a set of stochastic differential equations for the surface current vector. The joint PDF of (u, v) satisfies the Fokker-Planck equation,

$$\frac{\partial p}{\partial t} = \left(\frac{\Sigma^2}{2}\right)\left(\frac{\partial^2 p}{\partial u^2} + \frac{\partial^2 p}{\partial v^2}\right) + \frac{\partial}{\partial u}\left[\left(\frac{K}{h^2}u\right)p\right] + \frac{\partial}{\partial v}\left[\left(\frac{K}{h^2}v\right)p\right], \tag{17}$$

which is a linear second-order partial differential equation with the depth scale (h) taken as a constant. Transforming from the orthogonal coordinates (u, v) to the polar coordinates (w, φ) respectively the current speed and direction,

$$u = w\cos\varphi, \quad v = w\sin\varphi. \tag{18}$$

[11] The joint PDF of (u, v) is transformed into the joint PDF of (w, φ),

$$p(u, v)dudv = p(u, v)wdwd\varphi = \tilde{p}(w, \varphi)dwd\varphi. \tag{19}$$

[12] Integration of (19) over the angle φ from 0 to 2π yields the marginal PDF for the current speed alone,

$$p(w) = \int_0^{2\pi} \tilde{p}(w, \varphi)d\varphi. \tag{20}$$

[13] For a constant eddy viscosity (K) at $z = -h$, the steady state solution of equation (17) is given by

$$p(u,v) = A\exp\left[-\frac{K}{\Sigma^2 h^2}\left(u^2+v^2\right)\right], \tag{21}$$

where A is a normalization constant. Substitution of (21) into (19) and use of (20) yield

$$p(w) = 2\pi A w \exp\left(-\frac{Kw^2}{\Sigma^2 h^2}\right), \tag{22}$$

with

$$\int_0^\infty p(w)dw = 1. \tag{23}$$

[14] Substitution of (22) into (23) leads to the Rayleigh distribution

$$p(w) = \frac{2w}{a^2}\exp\left[-\left(\frac{w}{a}\right)^2\right], \quad a \equiv \frac{\Sigma h}{\sqrt{K}}, \tag{24}$$

with the scale parameter a. The basic postulation of constant K may not be met always at the upper ocean. Hence we require a model that can meet the twin objectives of (a) accommodating Rayleigh distribution whenever the basic hypothesis (constant K) that justifies it is satisfied and (b) fitting data under more general conditions. This requirement is supposed to be satisfied by the Weibull probability density function,

$$p(w) = \frac{b}{a}\left(\frac{w}{a}\right)^{b-1}\exp\left[-\left(\frac{w}{a}\right)^2\right], \tag{25}$$

where the parameters a and b denote the scale and shape of the distribution. This distribution has been recently used in investigating the ocean model predictability by *Ivanov and Chu* [2007a, 2007b].

4. Parameters of Weibull Distribution

[15] The four parameters (mean, standard deviation, skewness, and kurtosis) of the Weibull distribution are calculated by [*Johnson et al.*, 1994]

$$\text{mean}(w) = a\Gamma\left(1+\frac{1}{b}\right), \tag{26}$$

$$\text{std}(w) = a\left[\Gamma\left(1+\frac{2}{b}\right) - \Gamma^2\left(1+\frac{1}{b}\right)\right]^{1/2}, \tag{27}$$

$$\text{skew}(w) = \frac{\Gamma\left(1+\frac{3}{b}\right) - 3\Gamma\left(1+\frac{1}{b}\right)\Gamma\left(1+\frac{2}{b}\right) + 2\Gamma^3\left(1+\frac{1}{b}\right)}{\left[\Gamma\left(1+\frac{2}{b}\right) - \Gamma^2\left(1+\frac{1}{b}\right)\right]^{3/2}}, \tag{28}$$

$$\text{kurt}(w) = \frac{\Gamma\left(1+\frac{4}{b}\right) - 4\Gamma\left(1+\frac{1}{b}\right)\Gamma\left(1+\frac{3}{b}\right) + 6\Gamma^2\left(1+\frac{1}{b}\right)\Gamma\left(1+\frac{2}{b}\right) - 3\Gamma^4\left(1+\frac{1}{b}\right)}{\left[\Gamma\left(1+\frac{2}{b}\right) - \Gamma^2\left(1+\frac{1}{b}\right)\right]^2} - 3, \tag{29}$$

where Γ is the gamma function. The parameters a and b can be inverted [*Monahan*, 2006] from (26) and (27),

$$b \simeq \left[\frac{\text{mean}(w)}{\text{std}(w)}\right]^{1.086}, \quad a = \frac{\text{mean}(w)}{\Gamma(1+1/b)}. \tag{30}$$

[16] The skewness and kurtosis depend on the parameter b only [see (26) and (27)] for the Weibull distribution. The relationship between the kurtosis and skewness can be determined from (28) and (29).

5. Observational *w*-PDFs

[17] The data depicted in Section 2 are used to construct observational w-PDF (i.e., histograms) for the two stations (165°E, 110°W) along the equator in upper oceans (0–50 m) for the whole period (1990–2007), major El Nino events (May 91–Jul 92, Dec 92–Jun 93, Jul 94–Mar 95, May 97–Apr 98, May 02–Mar 03, Jul 04–Feb 05, Sep 06–Jan 07), and major La Nina events (Sep 95–Mar 96, Jul 98–Jun 00, Oct 00–Feb 01, Aug–Dec 07). It is found that the observational w-PDF fit the two-parameter Weibull distribution reasonably well in all occasions (Figure 1). At 165°E (western Pacific) the w-PDF has a largest peakedness with a lower mode (0.25 m s^{-1}) during the La Nina events, a medium peakedness for the whole period, and smallest peakedness with a higher mode (0.4 m s^{-1}) during the El Nino events; and vice versa at 110°W (eastern Pacific), the w-PDF has a largest peakedness with a lower mode (0.4 m s^{-1}) during the El Nino events, a medium peakedness for the whole period, and smallest peakedness wit a higher mode (0.65 m s^{-1}) during the La Nina events. From the western to eastern Pacific, the mode is comparable (0.4 m s^{-1}) during the El Nino events, and increases from 0.25 m s^{-1} to 0.65 m s^{-1} during the La Nina event. Such flip pattern of w-PDF between the eastern and western Pacific during El Nino/La Nina events may imply the importance of equatorial current systems in the El Nino-Southern Oscillation phenomenon.

[18] The four parameters (mean, standard deviation, skewness, and kurtosis) can also be calculated from the observational data (w),

$$\text{mean(w)} = \frac{1}{N}\sum_{i=1}^{N} w_i, \quad \text{std(w)} = \sqrt{\text{mean}[w-\text{mean}(w)]^2},$$
$$\text{skew}(w) = \frac{\text{mean}\left\{[w-\text{mean}(w)]^3\right\}}{\text{std}^3(w)},$$
$$\text{kurt}(w) = \frac{\text{mean}\left\{[w-\text{mean}(w)]^4\right\}}{\text{std}^4(w)} - 3, \tag{31}$$

for any location (station, depth) where the ADCP measurements were taken. Thus, a four-parameter dataset has been established each location. The scatter diagrams are drawn for all six stations (147°E, 156°E, 165°E, 170°W, 140°W,

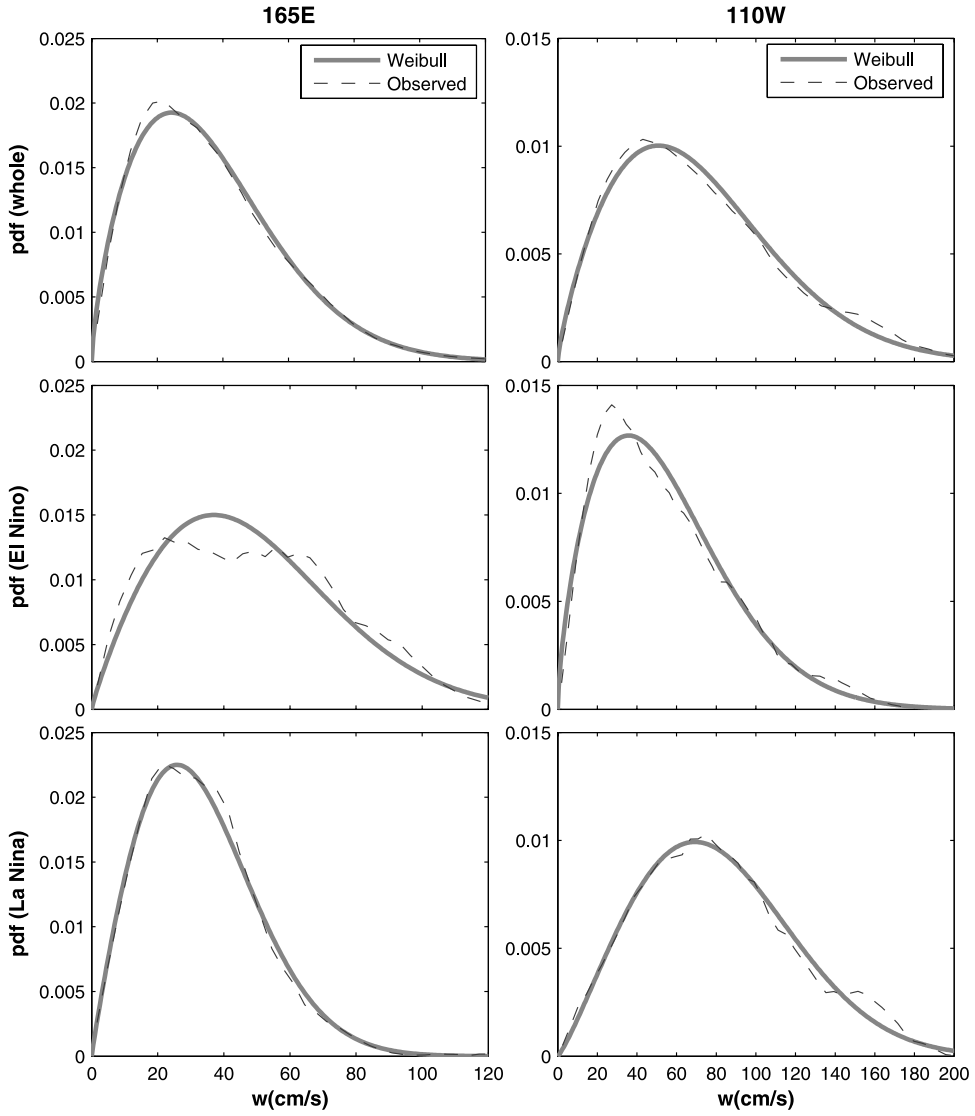

Figure 1. Comparison between observational w-PDFs (i.e., histogram, dashed curve) constructed from the TAO-ADCP data and Weibull distributions (solid curve) for upper layer (0–50 m) along the equator at: (left) 165°E, and (right) 110°W with the upper panels for the whole period, the middle panels for the major El Nino events, and the lower panels for the major La Nina events.

and 110°W) along the equator in upper oceans (0–50 m) and sub-layer (100–200 m) for the whole period (1990–2007), and El Nino/La Nina events. We may use the relationships between the skewness and the mean/std ratio (representing the parameter b, Figure 2) and between the kurtosis and the skewness (Figure 3) to identify the fitness of the Weibull distribution for observational w-PDFs for the whole period and the El Nino/La Nina events. The solid curve on Figures 1–3 shows the relationship for a Weibull variable.

[19] For the observational w-PDF in the upper layer (0–50 m), the skew(w) is evidently a concave function of the ratio mean(w)/std(w) (the same as the Weibull distribution), such that the theoretical function is positive for small values of this ratio and negative for large values. However, the ratio mean(w)/std(w) is always less than 2 for the whole period and El Nino events, and less than 2.5 for the La Nina events. The skewness is generally positive in the upper tropical Pacific for all occasions (Figure 2, top). Similarly, the relationship between skew(w) and kurt(w) in the observations is also similar to that for a Weibull variable (Figure 3). The agreement between the moment relationships in the upper layer (0–50 m) TAO-ADCP data and those for a Weibull variable reinforces the conclusion that these data are Weibull to a good approximation, which is not affected by the large-scale processes such as El Nino and La Nina events.

[20] The scatter diagrams of skew(w) versus ratio mean(w)/std(w) and kurt(w) versus skew(w) for the sub-layer (100–200 m) (bottom plots of Figures 2 and 3) show that the w-PDF for the lower layer (100–200 m) does not fit the Weibull distribution so well as the upper layer. Evident difference is found between the observational w-PDF and the Weibull distribution. Such difference can be explained as follows. For the upper layer, the horizontal velocity satisfies (9) and (10). This leads to that the current speed

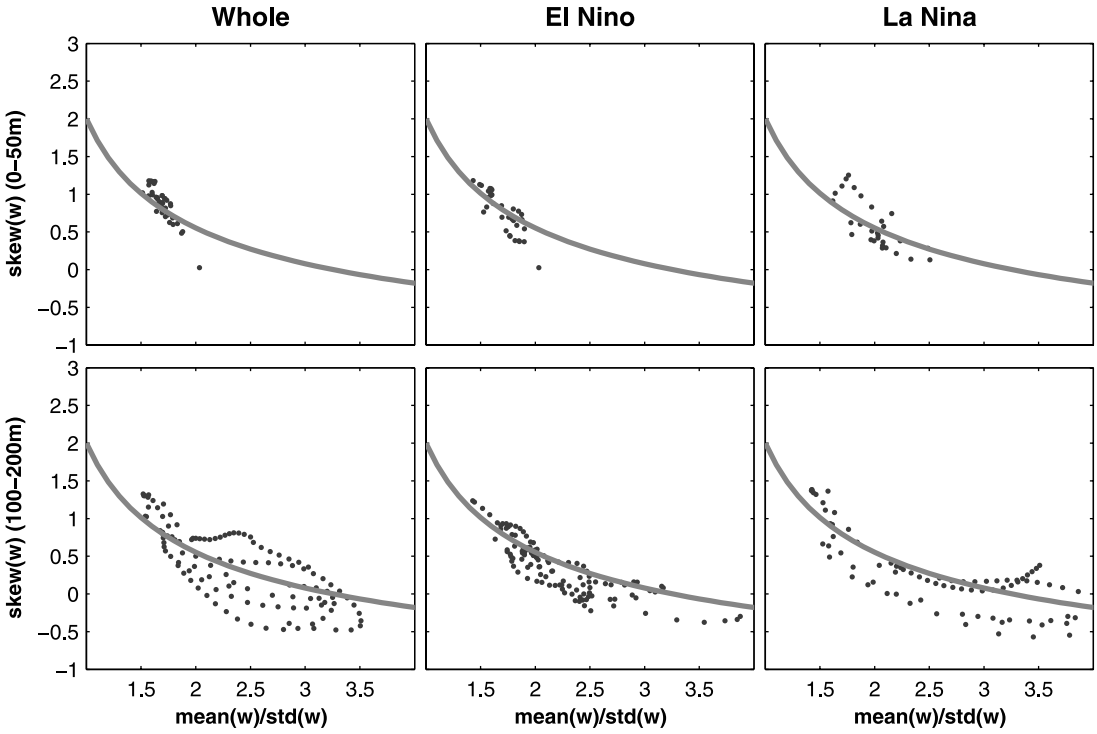

Figure 2. Relationship between the ratio mean(w)/std(w) and skew(w) for the observational w-PDFs (dots) from TAO-ADCP at the six stations and the Weibull distribution (solid curve) during (left) the whole period, (middle) major El Nino events, and (right) major La Nina events with the upper panels for the upper layer (0–50 m), and the lower panels for the sub-layer (100–200 m).

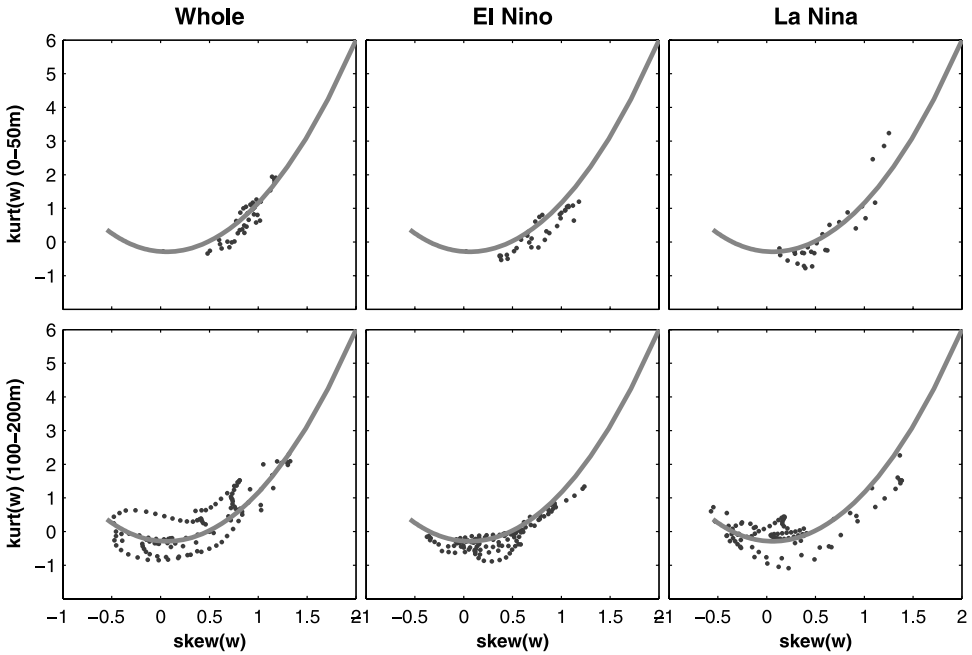

Figure 3. Relationship between kurt(w) and skew(w) for the observational w-PDFs (dots) from TAO-ADCP at the six stations and the Weibull distribution (solid curve) during (left) the whole period, (middle) major El Nino events, and (right) major La Nina events with the upper panels for the upper layer (0–50 m), and the lower panels for the sub-layer (100–200 m).

(w) satisfies the Rayleigh distribution for the constant eddy viscosity K and may extend to more general Weibull distribution for non-constant K. For the lower layer, the horizontal velocity does not satisfy (9) and (10). This may cause the deviation of w-PDF from the Weibull distribution.

6. Conclusions

[21] This study has investigated the probability distribution function of the current speeds (w) in upper tropical Pacific observationally, using long-term (1990–2007) hourly ADCP data at six stations during the TAO project; and theoretically, using a stochastic model derived using boundary layer physics. The following results were obtained.

[22] (1) Probability distribution function of the current speeds (w) satisfies the two-parameter Weibull distribution in the upper tropical Pacific Ocean (0–50 m) and does not satisfy the two-parameter Weibull distribution in lower tropical Pacific (100–200 m). In the upper tropical Pacific with a constant eddy viscosity K, the probability distribution function satisfies a linear second-order partial differential equation (i.e., the Fokker-Planck equation) with an analytical solution – the Rayleigh distribution (special case of the 2 parameter Weibull distribution). The stochastic differential equations are different between upper and lower layers in tropical Pacific (i.e., making the corresponding Fokker-Planck equation different), which causes the probability distribution function different.

[23] (2) The w-PDF in the upper ocean (0–50 m) satisfies the two-parameter Weibull distribution reasonably well all the time with different characteristics between El Nino and La Nina events. In the western Pacific, the w-PDF has a larger peakedness during the La Nina events than during the El Nino events; and vice versa in the eastern Pacific. From the western to eastern Pacific, the mode is comparable (0.4 m s^{-1}) during the El Nino events, and increases from 0.25 m s^{-1} to 0.65 m s^{-1} during the La Nina event. Such flip pattern of w-PDF between the eastern and western Pacific during El Nino/La Nina events may imply the importance of equatorial current systems in the El Nino-Southern Oscillation phenomenon.

[24] (3) Four moments of w (mean, standard deviation, skewness, kurtosis) have been characterized. It was found that the relationships between mean(w)/std(w) and skew(w) and between skew(w) and kurt(w) from the data are in fairly well agreement with the theoretical Weibull distribution for the upper (0–50 m) tropical Pacific for the whole period as well as El Nino/La Nina events, but are not in well agreement with the theoretical Weibull distribution for the lower (below 100 m depth) tropical Pacific. The ADCP data also show that the ratio mean(w)/std(w) is generally less than 2 for the whole period and El Nino events, and less than 2.5 for the La Nina events. The skewness is generally positive in the upper (0–50 m) tropical Pacific.

[25] (4) A primary motivation for the study of the probability distribution of upper layer ocean current speeds is the role these distributions play in the computation of spatially and/or temporally averaged horizontal fluxes of momentum, heat, water mass and chemical constituents. The Weibull distribution provides a good empirical approximation to the PDF of w, which is not affected by the large-scale processes such as El Nino and La Nina events. This presents the possibility of improving the representation of the horizontal fluxes that are at the heart of the coupled physical–biogeochemical dynamics of the marine system.

[26] **Acknowledgments.** The author would like to thank Chenwu Fan for invaluable comments and computational assistance, and the TAO Project Office of NOAA/PMEL for providing the ADCP data in tropical Pacific along the equator. The Office of Naval Research, Naval Oceanographic Office, and Naval Postgraduate School sponsored this research.

References

Galanis, G., P. Louka, P. Katsafados, G. Kallos, and I. Pytharoulis (2005), Applications of Kalman filters based on non-linear functions to numerical weather predictions, *Ann. Geophys.*, *24*, 2451–2460.

Gill, A. E. (1982), *Atmosphere-Ocean Dynamics*, 662 pp., Academic, San Diego, Calif.

Ivanov, L. M., and P. C. Chu (2007a), On stochastic stability of regional ocean models to finite-amplitude perturbations of initial conditions, *Dyn. Atmos. Oceans*, *43*, 199–225, doi:10.1016/j.dynatmoce.2007.03.001.

Ivanov, L. M., and P. C. Chu (2007b), On stochastic stability of regional ocean models with uncertainty in wind forcing, *Nonlinear Processes Geophys.*, *14*, 655–670.

Johnson, N., S. Kotz, and N. Balakrishnan (1994), *Continuous Univariate Distributions*, vol. 1, 756 pp., John Wiley, Hoboken, N. J.

Lozano, C. J., A. R. Robinson, H. G. Arrango, A. Gangopadhyay, Q. Sloan, P. J. Haley, L. Anderson, and W. Leslie (1996), An interdisciplinary ocean prediction system: Assimilation strategies and structured data models, in *Modern Approaches to Data Assimilation in Ocean Modeling*, edited by P. Malanotte-Rizzoli, Elsevier, Amsterdam.

Monahan, A. H. (2006), The probability distribution of sea surface wind speeds. part 1: Theory and SeaWinds observations, *J. Clim.*, *19*, 497–519.

McPhaden, M. J., et al. (1998), The Tropical Ocean–Global Atmosphere (TOGA) observing system: A decade of progress, *J. Geophys. Res.*, *103*, 14,169–14,240.

Pollard, R. T., and R. C. Millard (1970), Comparison between observed and simulated wind-generated inertial oscillations, *Deep Sea Res.*, *17*, 795–812.

P. C. Chu, Department of Oceanography, Naval Postgraduate School, Monterey, CA 93493, USA. (pcchu@nps.edu)